J|A|C|S COMMUNICATIONS

Published on Web 11/18/2010

Mixed Valency across Hydrogen Bonds

John C. Goeltz and Clifford P. Kubiak*

Department of Chemistry and Biochemistry, University of California—San Diego, 9500 Gilman Drive, M/C 0358, La Jolla, California 92093-0358, United States

Received September 30, 2010; E-mail: ckubiak@ucsd.edu

Abstract: An oxo-centered triruthenium cluster with one pyridine-4-carboxylic acid ligand forms a mixed valence monoanionic dicarboxylic acid dimer upon partial reduction. Dimerization is not observed in DMSO or in the deprotonated carboxylate complex. Infrared spectroscopy reveals the mixed valence dimer as a charge localized species, and UV/vis/NIR spectroscopy suggests a large stabilization of the ground state by mixed valency across hydrogen bonds, on the order of 2500 cm^{-1}, or 7 kcal/mol, relative to the hydrogen bonded but isovalent fully reduced dimer. The stabilization is a combination of hydrogen bonding and electronic coupling.

Mixed valency and proton-coupled electron transfer (PCET) are widely explored and relatively well understood fields,[1−9] but there are few reports from the intersection of the two.[10] There are many reported studies of photoinduced electron transfer across hydrogen bonds,[4,11−15] often yielding surprisingly large donor−acceptor couplings and a large range of observed kinetic isotope effects. Symmetric ground state electron transfer coupled to one or more protons would offer a platform for experimental insight into fundamental electron transfer, electron delocalization as a stabilizing factor for hydrogen bonds in self-assembly, the stability of hydrogen bonds in the presence of electron density, and the many multielectron multiproton transformations in natural and artificial photosynthesis.

Complex **1** (Figure 1), an oxo-centered trinuclear ruthenium cluster with one carbonyl, one pyridyl, and one isonicotinic acid ligand, affords multiple chromophores and oxidation states, as well as access to a simple hydrogen bonding motif, the head-to-head dicarboxylic acid dimer. Partial reduction of **1** results in the monoanionic dimer $(\mathbf{1})_2^-$ while full reduction gives a dianionic dimer, $(\mathbf{1})_2^{2-}$, each with a distinct electronic structure.

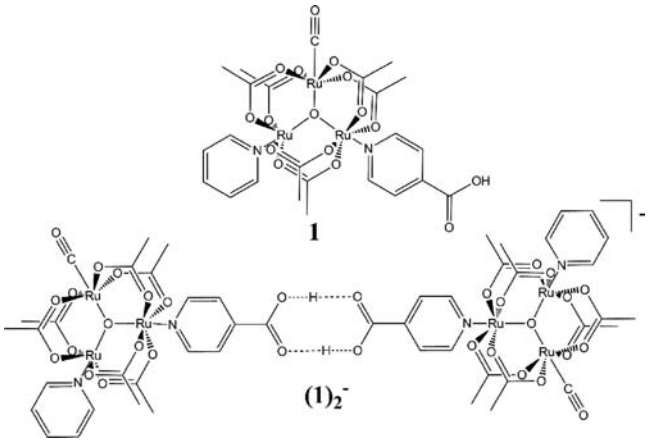

Figure 1. Structures of the isolated neutral ruthenium cluster **1** and the mixed valence dicarboxylic acid dimer $(\mathbf{1})_2^-$.

Previous studies predict electronic communication in reduced states of **1**, based on symmetry allowed interactions of the cluster dπ system with pyridine π^* orbitals.[16−18] Anodic reactions are found to be reversible one-electron processes in all cases, irrespective of solvent polarity and state of protonation (see Supporting Information). Figure 2 shows the cathodic electrochemistry of **1** in CH_2Cl_2 and DMSO. The reduction of the protonated cluster in CH_2Cl_2 (Figure 2, red solid line) shows two waves, and the reoxidation shows two waves with a larger apparent splitting. This can be explained by an ECE mechanism where E is a one-electron reduction and C is a reversible dimerization. Reduced cluster $\mathbf{1}^-$ reacts with neutral **1** in the diffusion layer to form a mixed-valence dimer $(\mathbf{1})_2^-$ which can then be reduced again to form a doubly reduced dimer $(\mathbf{1})_2^{2-}$, giving two reduction waves. This dimer is then reoxidized in two one-electron steps split symmetrically about the half wave potential of the monomer, resulting in waves of approximately half the peak current of the one-electron cluster oxidations seen at positive potentials. The neutral dimer falls apart to yield the neutral monomer **1**. Consistent with a dimerization step, the use of a solvent known to disrupt hydrogen bonding (DMSO, Figure 2, black dashed line) or use of the deprotonated cluster (Bu_4N^+ carboxylate salt, Supporting Information) results in a single reversible cathodic process with peak currents comparable to the anodic waves.

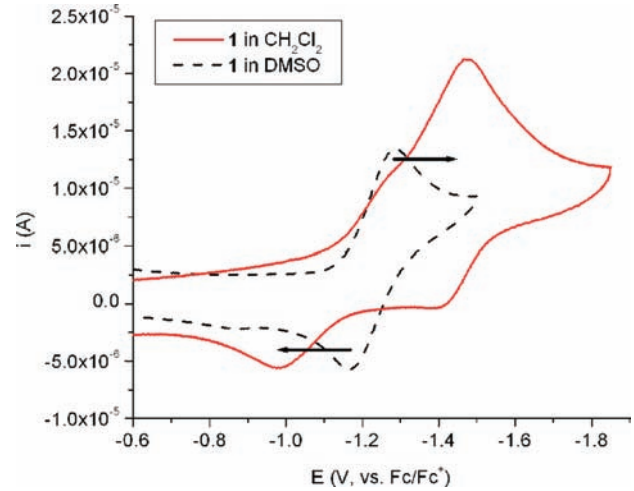

Figure 2. Cathodic electrochemistry of **1** in CH_2Cl_2 (red solid line) and DMSO (black dashed line), with arrows to indicate splitting of the reduction upon dimerization. ~1 mM with 0.1 M Bu_4NPF_6, Au WE, Pt CE, and Fc/Fc^+ REF.

The assignment of neutral **1** as a monomer and the reduced states as dimers is supported by diffusion coefficients measured by rotating disk voltammetry measurements on **1** and diffusion ordered NMR spectroscopy (DOSY) on neutral and reduced states of **1** (full details in Supporting Information). No neutral dimer is detected by IR,

10.1021/ja108841k

NMR, or rotating disk electrochemistry at millimolar concentrations in MeCN or CH_2Cl_2 supporting a $K_{dim} < 0.01$ for **1**. Another measure of thermodynamic stability, the comproportionation constant, can be calculated from the splitting in the reoxidation waves of $(\mathbf{1})_2^{2-}$. $K_c \approx 10^7$ for the mixed valence ion in CH_2Cl_2 indicating a highly stable mixed valence ion with respect to disproportionation. Significant contributions are expected from both electrostatic and electronic structure factors.[19] The electronic structures of the three oxidation states were probed by infrared and UV/vis/near IR spectroelectrochemistry, shown in Figure 3.

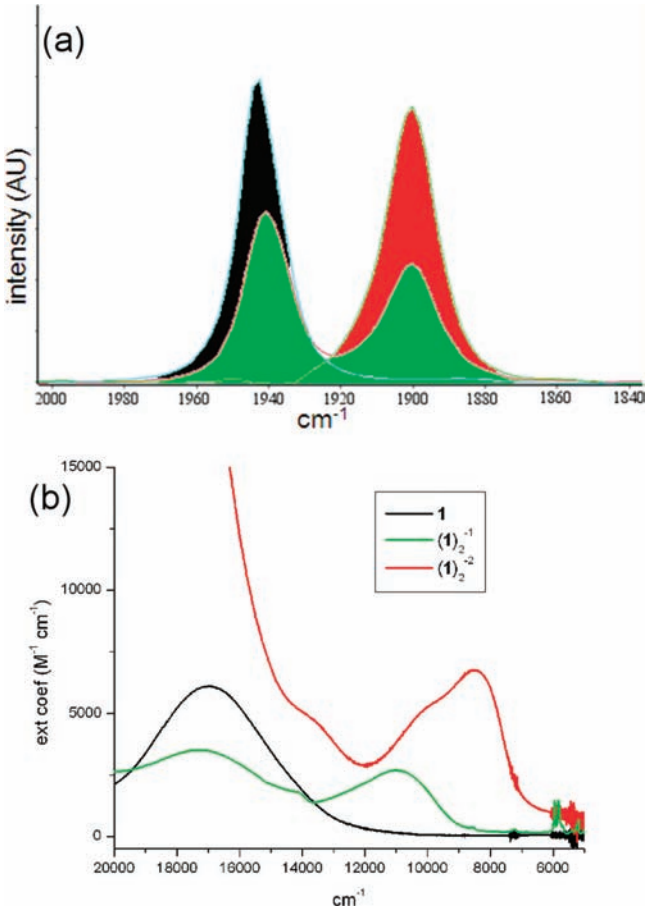

Figure 3. IR and UV/vis/NIR spectra of **1**, 3 mM in MeCN, −20 °C. (a) ν(CO) region of the infrared, showing electron localization on the IR time scale in the singly reduced mixed valence dimer (green). (b) UV/vis/NIR, showing a distinct electronic structure for the mixed valence dimer (green).

Figure 3a shows the ν(CO) region of the infrared. The neutral cluster shows the usual band at 1945 cm^{-1}, and a fully reduced sample shows a single band at 1900 cm^{-1} with the usual shift seen for a single reduction of a carbonyl substituted $Ru_3O(OAc)_6$ cluster. A half reduced sample shows a slight shift for the "neutral" band to about 1940 cm^{-1}, consistent with an increase in pyridine donor ability upon dimerization with a reduced cluster, but otherwise simply a superposition of the neutral and reduced species. This confirms an electron-localized structure, with an upper bound on the electron transfer rate constant (k_{ET}) of $\sim 10^{10}$ s^{-1}.

Figure 3b shows UV/vis/NIR spectra obtained as **1** is stepped through two one-electron reductions, with equivalent results obtained by either chemical or electrochemical reduction. The fully reduced cluster spectrum (red line) is similar to those of other reduced carbonyl substituted triruthenium clusters,[20,21] with several bands evident between 7000−12 000 cm^{-1} and an increase in intensity and blue shift of the intracluster band observed at 588 nm (17000 cm^{-1}) in the neutral species. The monoanionic species identified as $(\mathbf{1})_2^-$ exhibits an unusual spectral response, not simply the superposition of neutral and fully reduced spectra that might be expected in view of the simple weighted average of neutral and reduced ν(CO) bands in the infrared spectra in Figure 3a. The intracluster absorption decreases in intensity, as is seen in singly reduced dimers of triruthenium clusters bridged by pyrazine or 4-4′-bipyridine,[20] but the near-IR shows an absorption profile at much higher energy than the fully reduced dimer with a ν_{max} of 11 000 cm^{-1} (green trace) instead of 8500 cm^{-1} (red trace). Several possible explanations for the mixed valence electronic structure merit immediate discussion: orbital destabilization due to electron−electron repulsion, an exciton shift, a non-Gaussian Marcus−Hush intervalence charge transfer (IVCT) band, and a hypsochromic shift of the cluster-to-ligand charge transfer (CLCT) transitions due to stabilization of the ground state.

Red shifts upon sequential reduction similar in appearance to those in Figure 3b have been observed in CLCT transitions of trispyridyl triruthenium clusters.[22] This was attributed to destabilization of occupied cluster orbitals by increasing electron−electron repulsion. Applying this explanation to $(\mathbf{1})_2^{-/2-}$ would require sequential population of a single molecular orbital, and thus a delocalized Robin−Day Class III classification.[9] The IR spectra preclude a delocalized electronic structure (Figure 3a) and thus electronic occupancy as an explanation for the band positions in $(\mathbf{1})_2^-$ and $(\mathbf{1})_2^{2-}$.

An exciton shift might be invoked for $(\mathbf{1})_2^{2-}$ as a dimer of chromophores,[23] relative to $(\mathbf{1})_2^-$. However the exciton splitting falls off as the cube of the distance between the dipole moment centers[24,25] (∼14 Å for these dimers) and is calculated to be on the order of 50 cm^{-1} for these species, more than an order of magnitude lower than the observed 2500 cm^{-1} shift.

If the mixed valence dimer $(\mathbf{1})_2^-$ is moderately coupled and fits solidly in the Robin−Day Class II regime, a distinct electronic signature is expected in lieu of a weighted average of the neutral and doubly reduced spectra. This has been observed in a mixed valence hydrogen bonded assembly.[10] When the non-Gaussian absorption profile in the near-IR spectrum of $(\mathbf{1})_2^-$ is treated as a single IVCT transition, the electronic coupling, H_{ab}, and the total reorganization energy, λ, can be extracted using the measured transition dipole moment and Marcus−Hush theory.[1,26,27] Such treatment gives $H_{ab} = 370$ cm^{-1} and $\lambda = 11\,000$ cm^{-1} using a Ru−Ru distance of 14 Å for the electron transfer distance r_{ab}. The reorganization energy is in very good agreement with thermodynamic estimates for 0/− couples of triruthenium clusters.[16,28] The predicted line width at half-maximum is 4650 cm^{-1}, wider than the observed $\Delta\nu_{1/2}$ of 3600 cm^{-1}. However, the *half*-width at half maximum on the high energy side is 2325 cm^{-1}, half the predicted bandwidth. $H_{ab}/\lambda = 3\%$ appears too small to justify narrowing of an IVCT band, but H_{ab} may actually be larger if the electron transfer distance r is shorter than the Ru−Ru intercluster distance. The main problem with this line of reasoning is that it cannot explain the disappearance of the CLCT transitions from the cluster to the pyridine and isonicotinic acid ligands observed in $(\mathbf{1})_2^{2-}$ and in other anionic clusters of this type.

If the near IR absorption profile in $(\mathbf{1})_2^-$ is indeed two CLCT transitions (e.g., cluster-to-pyridine and cluster-to-isonicotinic acid) as it is in $(\mathbf{1})_2^{2-}$, the large hypsochromic shift can be explained as a stabilization of the ground state by mixed valency across hydrogen bonds. Stabilization of ground states by hydrogen bonding or ion pairing is well-known,[29−31] but the effect is not evident in the fully reduced species $(\mathbf{1})_2^{2-}$, confirmed as a dimer by diffusion NMR experiments. This means that the combination of hydrogen bonding

and mixed valency stabilizes the ground state of $(\mathbf{1})_2^-$ by ~2500 cm^{-1} (or 7.1 kcal/mol, or 310 meV).

$(\mathbf{1})_2^-$ is the best characterized system to date for exploration of proton-dependent or proton-coupled mixed valency, where in the latter case the electron transfer depends explicitly on the proton coordinate. A study is forthcoming with full solvent dependence of electrochemistry and electronic spectroscopy, variation of the electron donating ability of the ancillary pyridine ligand, and deuteration of the pyridine carboxylic acid. This work will illuminate the behavior of hydrogen bonded systems subjected to repeated electron transfer as well as stabilization of the hydrogen bonds by electron exchange.

Acknowledgment. We thank Starla Glover for many discussions of electron donor−acceptor interactions, Dr. Anthony Mrse in the UCSD NMR Facility for assistance with DOSY experiments, Matthew Millard for his help with low temperature NMR, and Dr. Yongxuan Su in the UCSD Molecular Mass Spectrometry Facility. We gratefully acknowledge support from NSF CHE-0616279.

Supporting Information Available: Full experimental details for synthesis, electrochemistry, and DOSY, and calculations of H_{ab}. This information is available free of charge via the Internet at http://pubs.acs.org.

References

(1) Brunschwig, B. S.; Creutz, C.; Sutin, N. *Chem. Soc. Rev.* **2002**, *31*, 168–184.
(2) Lebeau, E. L.; Binstead, R. A.; Meyer, T. J. *J. Am. Chem. Soc.* **2001**, *123*, 10535–10544.
(3) Cukier, R. I.; Nocera, D. G. *Annu. Rev. Phys. Chem.* **1998**, *49*, 337–369.
(4) Derege, P. J. F.; Williams, S. A.; Therien, M. J. *Science (Washington, DC, U.S.)* **1995**, *269*, 1409–1413.
(5) Mayer, J. M. *Annu. Rev. Phys. Chem.* **2004**, *55*, 363–390.
(6) Sjodin, M.; Styring, S.; Akermark, B.; Sun, L. C.; Hammarstrom, L. *J. Am. Chem. Soc.* **2000**, *122*, 3932–3936.
(7) Hammes-Schiffer, S. *Acc. Chem. Res.* **2001**, *34*, 273–281.
(8) Marcus, R. A. *Annu. Rev. Phys. Chem.* **1964**, *15*, 155.
(9) Robin, M. B.; Day, P. *Adv. Inorg. Chem. Radiochem.* **1967**, *10*, 247.
(10) Sun, H.; Steeb, J.; Kaifer, A. E. *J. Am. Chem. Soc.* **2006**, *128*, 2820–2821.
(11) Hsu, T. L. C.; Engebretson, D. S.; Helvoigt, S. A.; Nocera, D. G. *Inorg. Chim. Acta* **1995**, *240*, 551–557.
(12) Papoutsakis, D.; Kirby, J. P.; Jackson, J. E.; Nocera, D. G. *Chem.—Eur. J.* **1999**, *5*, 1474–1480.
(13) Sessler, J. L.; Sathiosatham, M.; Brown, C. T.; Rhodes, T. A.; Wiederrecht, G. *J. Am. Chem. Soc.* **2001**, *123*, 3655–3660.
(14) Kurlancheek, W.; Cave, R. J. *J. Phys. Chem. A* **2006**, *110*, 14018–14028.
(15) Betts, J. N.; Beratan, D. N.; Onuchic, J. N. *J. Am. Chem. Soc.* **1992**, *114*, 4043–4046.
(16) Goeltz, J. C.; Benson, E. E.; Kubiak, C. P. *J. Phys. Chem. B* **2010**, *114*, 14729–14734.
(17) Goeltz, J. C.; Hanson, C. J.; Kubiak, C. P. *Inorg. Chem.* **2009**, *48*, 4763–4767.
(18) Salsman, J. C.; Ronco, S.; Londergan, C. H.; Kubiak, C. P. *Inorg. Chem.* **2006**, *45*, 547–554.
(19) Richardson, D. E.; Taube, H. *Coord. Chem. Rev.* **1984**, *60*, 107–129.
(20) Ito, T.; Hamaguchi, T.; Nagino, H.; Yamaguchi, T.; Kido, H.; Zavarine, I. S.; Richmond, T.; Washington, J.; Kubiak, C. P. *J. Am. Chem. Soc.* **1999**, *121*, 4625–4632.
(21) Abe, M.; Sasaki, Y.; Yamada, Y.; Tsukahara, K.; Yano, S.; Yamaguchi, T.; Tominaga, M.; Taniguchi, I.; Ito, T. *Inorg. Chem.* **1996**, *35*, 6724–6734.
(22) Baumann, J. A.; Salmon, D. J.; Wilson, S. T.; Meyer, T. J.; Hatfield, W. E. *Inorg. Chem.* **1978**, *17*, 3342–3350.
(23) Kobayashi, N.; Lam, H.; Nevin, W. A.; Janda, P.; Leznoff, C. C.; Lever, A. B. P. *Inorg. Chem.* **1990**, *29*, 3415–3425.
(24) Kasha, M. *Radiat. Res.* **1963**, *20*, 55–71.
(25) Osuka, A.; Maruyama, K. *J. Am. Chem. Soc.* **1988**, *110*, 4454–4456.
(26) D'Alessandro, D. M.; Keene, F. R. *Chem. Rev.* **2006**, *106*, 2270–2298.
(27) D'Alessandro, D. M.; Keene, F. R. *Chem. Soc. Rev.* **2006**, *35*, 424–440.
(28) Londergan, C. H.; Salsman, J. C.; Lear, B. J.; Kubiak, C. P. *Chem. Phys.* **2006**, *324*, 57–62.
(29) Rodionova, G. N.; Krutovskaya, I. V.; Rodionov, A. N.; Tuchin, Y. G.; Karpov, V. V. *J. Appl. Spectrosc.* **1980**, *32*, 344–348.
(30) Piotrowiak, P.; Kobetic, R.; Schatz, T.; Strati, G. *J. Phys. Chem.* **1995**, *99*, 2250–2253.
(31) Skoog, D. A.; Holler, J. F.; Nieman, T. A. *Principles of Instrumental Analysis*, 5th ed.; Harcourt Brace and Company: Orlando, 1998.

JA108841K